Research on Forming Quality of GH4169 Superalloy Multi-Step Hollow Turbine Shaft by Three-roll Skew Rolling

Si-Yuan Chen[1,2], Xue-Dao Shu[1,2,*], Yong-Ming Xu[1,2], Qian Chen[1,2], Hai-Jie Xu[1,2], Bao-Shou Sun[1,2], Ying Wang[1,2] and Yi-Min Deng[1,2]

[1]*Faculty of Mechanical Engineering and Mechanics, Ningbo University, Ningbo City 315211, China*

[2]*Zhejiang Provincial Key Lab of Part Rolling Technology, Ningbo City 315211, China*

Abstract: This paper innovatively proposes a three-roll skew rolling process for flexible forming of hollow turbine shaft, which solves the problems of long manufacturing process and low material utilization of hollow turbine shaft, the core component of aeroengine. Simufact.Forming 14.0 (SF) numerical simulation software was used to establish the finite element model of two-pass three-roll skew rolling of the GH4169 superalloy turbine shaft. The effects of process parameters on the outer diameter error, roundness error and wall thickness uniformity of the rolled piece were investigated by single factor experiments. A five-factor three-level orthogonal test was designed to explore the optimum process parameters by 'comprehensive scoring method'. The results show that the optimal process parameters are that the first pass roll rotating speed is 40 rad/min, the first pass axial speed is 15 mm/s, the second pass roll rotating speed is 50 rad/min, the second pass axial speed is 25 mm/s, and the billet preheating temperature is 1000ºC. The axial velocity of the second pass has the greatest influence on the test results, while the rotational speed of the second pass has the least influence. Under the optimal parameter combination simulation experiment, the outer diameter error, outer roundness error and wall thickness standard deviation are 0.151 mm, 0.121 mm and 0.034 mm, respectively, which are better than the results in the orthogonal test table. The research results provide a theoretical basis for realizing flexible, economical and high-quality forming of hollow turbine shaft by three-roll skew rolling.

Keywords: Skew rolling, Two-step deforming, Process parameter, Finite element simulation, Flexible forming.

1. INTRODUCTION

As one of the core components of aircraft engine, the turbine shaft has high demands on its mechanical properties and forming quality. At present, the main method of turbine shaft forming is still the traditional forging process, which has the defects of insufficient mold versatility, cumbersome forming process and low production efficiency. The three-roll skew rolling flexible forming process has the advantages of significantly reducing rolling load, saving equipment space, and improving mold versatility [1]. In terms of the forming quality of rolled pieces, Japanese scholar K. Nakasuji *et al*. verified the feasibility of forming hollow tubes on a three-roll skew mill, and studied the forming quality and forming law of rolled pieces in terms of dimensional accuracy and wall thickness uniformity in detail [2]. Z. Pater's team validated the feasibility of applying three-roll skew rolling technology to the production of light truck TC4 hollow shafts based on numerical simulation results (shape of the rolled piece, wall thickness distribution, equivalent strain, and changes in rolling force and torque during the rolling process) [3-4]. Polish scholar A. Stefanik *et al*. determined the distribution of stress, strain and temperature during the

rolling process by finite element analysis of 1050A aluminum rods with a diameter of 20 mm and 1050A and 2017A aluminum rods with a diameter of 25 mm formed by three-roll skew rolling process. Finally, the results of theoretical and numerical simulation were verified by experiments [5-6]. J. H. Min [7] compared the rolling process of three special grooves in three-roll skew rolling by finite element simulation, and investigated the influence of process parameters such as roll radius, rolling speed and rolling temperature on the shape change of rolled pieces. Lv Qinggong found that the eccentric defect of the wall thickness of the raw pipe can be effectively reduced by increasing the wall reduction, roller speed and reducing the rolling temperature during the rolling process [8]. A large number of scholars have explored the effects of three-roll skew rolling process parameters on metal forming [9-12]. The flexible forming theory of three-roll skew rolling of hollow shaft is systematically expounded by Shu Xuedao's team of Ningbo University, and the feasibility of three-roll skew rolling of hollow axle is expounded by combining theory with experiments [13]. The above research works provide technical support for three-roll skew rolling of multi-step hollow turbine shaft.

This paper presents a two-pass three-roll skew rolling process for GH4169 superalloy multi-step hollow turbine shaft. Using Simufact.Forming (SF) finite element simulation software, the influence of process

*Address correspondence to this author at the Faculty of Mechanical Engineering and Mechanics, Ningbo University, Ningbo City 315211, China; Tel: +8613957878831; E-mail: shuxuedao@nbu.edu.cn

parameters (roll rotating speed, axial speed, Billet preheating temperature)on the forming quality was explored .Then through the orthogonal experiment, the optimal combination of parameters and the order of influence are obtained, and the optimal parameter combination is numerically simulated to verify the reliability of the orthogonal experiment.

2. METHODOLOGY

2.1. Forming Principle of Three-Roll Skew Rolling

As shown in Figure **1**, it is the schematic diagram of the three-roll skew rolling forming turbine shafts. The three rollers rotating in the same direction are distributed around the rolling center line at 120° circumference, and the roll axis is deflected by a certain angle relative to the rolling center line (feed angle). The rolling piece is driven by the rollers to make a spiral forward movement, and the forming requirements of the multi-step turbine shaft are realized by controlling the roll spacing of the three rolls. In order to ensure the accuracy and stability of the forming process, the rolling speed is adjusted by the active traction of the chuck.
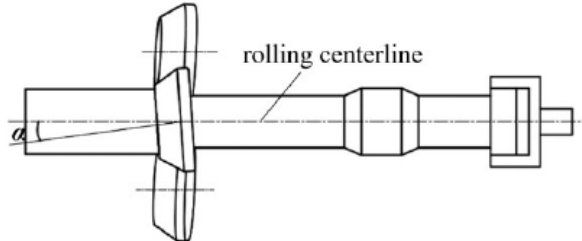
Figure 1: Schematic diagram of three-roll skew rolling forming turbine shafts.

2.2. Finite Element Model

Figure **2** is the finite element model of three-roll skew rolling forming turbine shafts, which mainly includes three rolls with the same sizes, tube blank, mandrel and chuck.
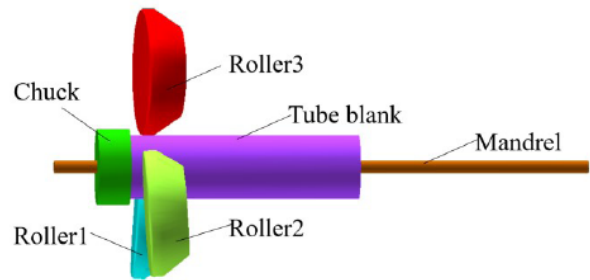
Figure 2: Finite element model of three-roll skew rolling forming turbine shafts.

The material of turbine shaft is GH4169 superalloy, which is made of turbine shaft, turbine blade, turbine disk and other main components in aero-engines [14]. Its elemental composition is shown in Table **1**. The constitutive equation used in this paper is as follows [15]:

$$\varepsilon = 2.46748 \times 10^{18}[\sinh(0.00346\sigma)]^{4.95225}\exp(\frac{-505649}{RT}) \quad (1)$$

Where ε is the plastic stress rate /s^{-1}; σ is the peak stress; R is the gas constant (8,314 J·mol^{-1}·K^{-1}), and T is the temperature.

To ensure the correctness of the premise of convenient research, the actual proportion of the step shaft is reduced to 1/3 of the original, and its parameters are shown in Figure **3**.
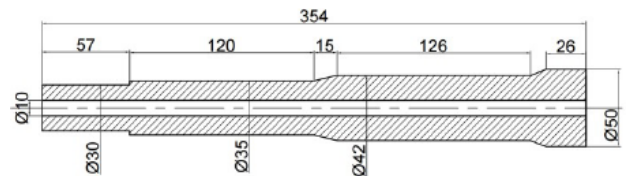
Figure 3: Turbine shaft size diagram.

In order to form the turbine shaft shown in Figure **3**, the tube blank with the outer diameter of 50 mm, the inner diameter of 10 mm and a length of 230 mm was selected for rolling. The blank is divided into 3mm by hexahedral mesh, and Step shaft with a diameter of 30 mm meshed to 1/8 of the normal area. In order to avoid the phenomenon of mesh distortion in the simulation

Table 1: Elemental composition of alloy GH4169 (in wt. pct)

C	Cr	Ni	Mo	Al	Co	Nb	Ti
0.037	18.31	52.51	3.05	0.56	0.26	5.25	1.01
Cu	**Co**	**Mn**	**Si**	**S**	**P**	**Mg**	**Fe**
≤0.30	≤1	≤0.35	≤0.35	≤0.015	≤0.015	≤0.01	Remainder

process [16-17], the author takes the strain change of 0.4 as the standard of remeshing, and automatically determines and remeshes the distorted mesh in SF. The initial and boundary conditions are given in Reference [18].

2.3. Technical Parameter

Table **2** shows the main dimension parameters of three-roll skew rolling model of multi-step turbine shaft.

Table 2:   **Model Parameter**

Model Parameter	Unit	Value
Maximum roll diameter D	mm	100
Length of reduction area L1	mm	25
Length of forming area L2	mm	12
Roll length L	mm	37
Taper angle of reducing area	°	30
Feed angle	°	5
Outside diameter of tube blank	mm	50
Inner diameter of tube blank	mm	50

Because GH4169 is a typical difficult-to-machine material, the process plasticity is poor [19]. The author uses two passes to form the turbine shaft. As shown in Figure **4**, the forming process of the turbine shaft is 6mm in the first pass, and the neck reductions of the three steps in the second pass are 2mm, 9mm and 14mm respectively.
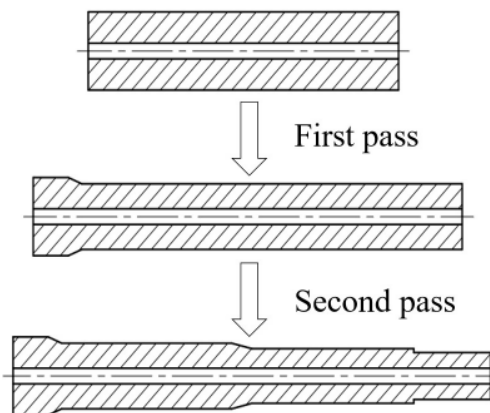

Figure 4: Two-pass forming process of three-roll skew rolling forming turbine shafts.

3. ANALYSIS OF INFLUENCE FACTORS ON FORMING QUALITY OF THREE-ROLL SKEW ROLLING FOR TURBINE SHAFT

In turbine shaft forming, transverse deformation and metal reflow often occur, which will greatly affect the final forming accuracy of turbine shaft. As shown in Figure **5**, the metal in the A region is affected by the roll, and the velocity component is obviously opposite to the rolling direction, and the maximum value is -22.49 mm/s, which leads to the phenomenon of metal backflow. Wrong process parameters will lead to increased local deformation of rolled pieces, external surface distortion, and even lead to blistering, bell mouth, tail triangle and other defects. The author explores the effect of process parameters on the forming quality of turbine shaft by single factor analysis, which provides an important reference for optimizing process parameters and improving forming defects.
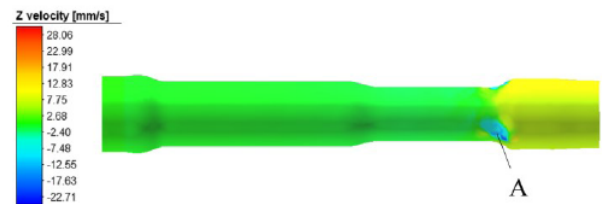

Figure 5: Axial velocity field of metal.

3.1. Determination of Analysis Indexes and Process Parameters

The equal-diameter sections of three steps on the turbine shaft are selected as the research object, and the position diagram of the sampling surfaces are shown in Figure **6**(**a**). According to the length and outer diameter of the equal diameter section, 7 sampling surfaces of the first step shaft and the second step shaft and 4 sampling surfaces of the third step shaft are taken respectively. The sampling points on each surface are shown in Figure **6**(**b**).

In this paper, the outer diameter error, outer surface roundness error and wall thickness uniformity of the rolled piece after simulation are selected as the analysis indicators of the turbine shaft forming quality. The outer diameter error refers to the absolute difference between the actual outer diameter d_i of each section of the rolled piece and its corresponding target outer diameter d:

$$e_i = |d_i - d| \tag{2}$$

Roundness is an important index to evaluate the forming quality of shaft parts. The sampling point is defined in S.F by the sampling method in Figure **6**, and the outer roundness error of the rolled piece is calculated by the least square circle method [20]. Finally, the average value δ of the outer surface roundness error of the formed part is obtained.
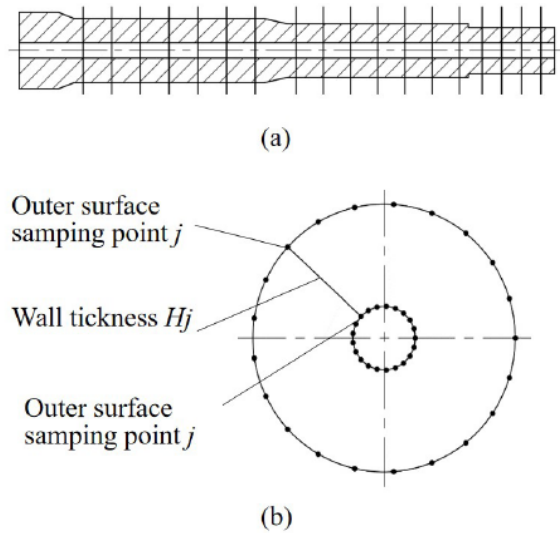
Figure 6: Sampling scheme (**a**) Sampling sections and (**b**) Section sampling points.

Considering that the eccentricity of the inner and outer rings may occur when the roundness error of the rolled piece is small, the wall thickness uniformity is introduced as the evaluation index, so as to more comprehensively explore the influence of process parameters on the forming quality of the rolled piece. As shown in Figure **6**(**b**), the wall thickness H_j is obtained by calculating the distance between the corresponding nodes of the inner and outer rings of the cross section. The wall thickness uniformity of the cross section of the rolled piece is measured according to the standard deviation of the wall thickness. The smaller the value is, the more uniform the wall thickness of the rolled piece is. The specific calculation formula is as follows:

$$H_j = \sqrt{\left(X_j - x_j\right)^2 + \left(Y_j - y_j\right)^2} \tag{3}$$

$$\overline{H_j} = \frac{1}{n}\sum_{j=1}^{n} H_j \tag{4}$$

$$\sigma_j = \sqrt{\frac{1}{n}\sum_{j=1}^{n}\left(H_j - \overline{H_j}\right)^2} \tag{5}$$

$\left(X_j, Y_j\right)$ is the coordinate value of j sampling point on the outer surface of the section.; $\left(x_j, y_j\right)$ is the coordinate value of j sampling point on the inner surface of the section; $\overline{H_j}$ is the average wall thickness of the section; n is the wall thickness on each section. The wall thicknesses on the three steps are shown in Figure **3**, which are 21 mm, 17 mm and 15 mm, respectively.

Table 4: Evaluation Index of Forming Quality

Quality Indexs	Designations
Outer diameter error	e
Surface roundness error	δ
Wall thickness standard deviation	σ

In the two-pass forming process of the turbine shaft, the speed matching between the two passes will greatly affect the forming quality of the rolled piece, while the rolling temperature also has an important significance to the rolling process, which not only affects the macroscopic forming quality of the rolled part but also has an effect on the microstructure of the rolled part [21]. Therefore, this paper focuses on the influence of the first pass roll rotating speed n1, the first pass axial speed v1, the second pass roll rotating speed n2, the second pass axial speed v2 and the billet preheating temperature T on the quality of the rolled piece. A total of 25 groups of experiments were set up through the single factor experimental scheme of 5 factors and 5 levels, as shown in Table **3**. Outer diameter error, external roundness error and wall thickness standard deviation are selected as the results of the study, the names are simplified in this chapter chart, as shown in Table **4**.

Table 3: Process Parameter Setting Scheme and Test Results

Parameters	Designations	Reference Section	Change Section
First pass roll rotating speed（rad·min^{-1}）	n1	80	40/60/80/100/120
First pass axial speed（mm·s^{-1}）	v1	20	10/15/20/25/30
Second pass roll rotation speed（rad·min^{-1}）	n2	60	40/50/60/70/80
Second pass axial feed speed（mm·s^{-1}）	v2	20	10/15/2/25/60
Billet preheating temperature（°C）	T	1050	950/1000/1050/1100/115

3.2. Effect of First Pass Roll Rotating Speed on Forming Quality

Figure **7** shows the influence curves of n1 on the outer diameter error, outer surface roundness error and wall thickness uniformity of the rolled piece.
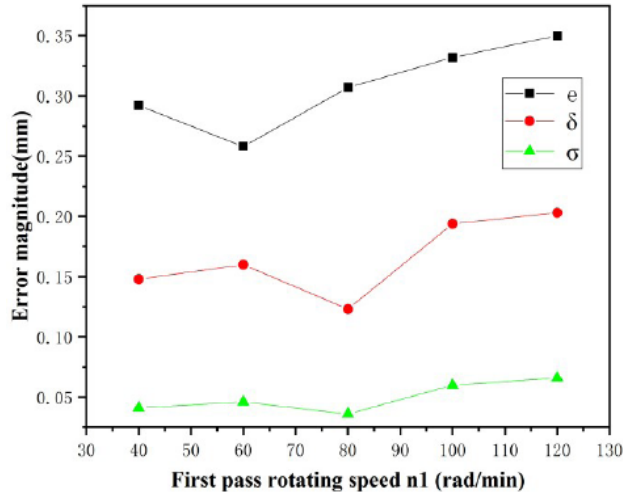

Figure 7: Effects of the first pass rotating speed on forming quality.

The outer diameter error of rolled piece decreases first and then increases with the increase of n1. When the n1 is 60 rad/min, the outer diameter error of the rolled piece reaches the minimum value of 0.258 mm, which indicates that the outer diameter of the rolled piece under this speed condition is most in line with the target value. When n1 increases from 60 rad/min to 120 rad/min, the outer diameter error of the rolled piece gradually increases, but the increase rate slows down.

The roundness error and the wall thickness standard deviation of the rolled piece show increasing trends with the increase of n1, and the increase rate is relatively stable. Both of them have an inflection point at the speed of 80 rad/min where the minimum roundness error of the rolled piece is 0.123 mm, and the minimum standard deviation of the wall thickness is 0.036 mm, indicating that the shape of the outer ring of the rolled piece under this speed condition is the closest to the circle and the wall thickness of the rolled piece under this speed condition is the most uniform.

The experimental data show that increasing the roll speed appropriately within a certain range is beneficial to improve the outer diameter accuracy of the rolled piece, but with the further increase of n1, the stability of the metal deformation will decrease. The number of rolling times per unit time increases, which can improve the forming quality of rolled pieces to a certain extent. However, the increase of rotational speed will also increase the fluidity of the rolled metal [3], making the lateral additional deformation and backflow of the metal more obvious.

3.3. Effect of First pass Axial Speed on Forming Quality

It can be seen from Figure **8** that the outer diameter error of the rolled piece gradually increases with the increase of the axial speed in the first pass (v1). When the v1 is 10 mm/s, the outer diameter error of the rolled piece is the minimum of 0.246 mm. With the increase of v1, the metal flowability of the rolled piece increases, especially the amount of reflow metal along the axial direction, which makes the outer diameter of the rolled piece larger than the target value.
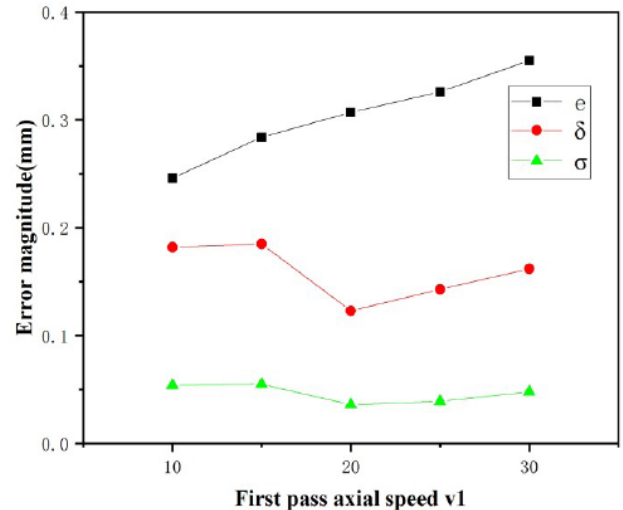

Figure 8: Effects of the first pass axial speed on forming quality.

The roundness error of the rolled piece decreases first and then increases with the increase of v1. When the axial velocity is 20 mm/s, the minimum value appears, and the roundness error of the rolled piece is 0.123 mm. The variation trend of wall thickness uniformity is similar to that of the external roundness error, and the minimum value of the wall thickness standard deviation is 0.036 mm when the v1 is 20 mm/s.

Considering comprehensively, appropriately increasing the axial velocity of the first pass can reduce the roundness error and wall thickness standard deviation of the rolled piece to a certain extent, but it should not be too large.

3.4. Effect of Second Pass Roll Rotating Speed on Forming Quality

Figure **9** shows the influence curve of the second pass roll rotating speed (n2) on the outer diameter error, external roundness error and wall thickness uniformity of the rolled piece.
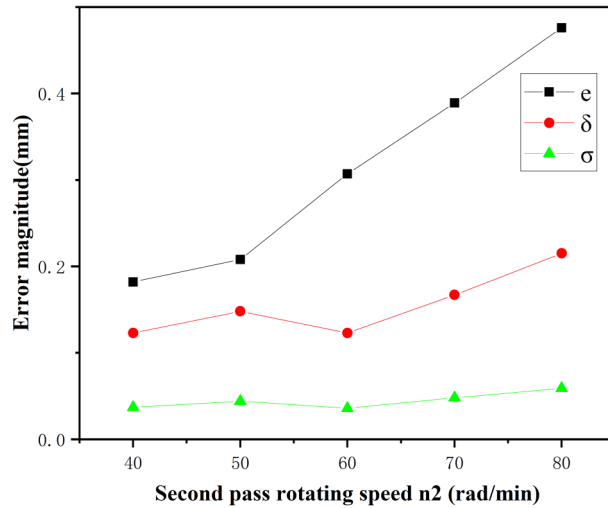

Figure 9: Effects of the second pass rotating speed on forming quality.

It can be seen from Figure **9** that the outer diameter error of the rolled piece increases gradually with the increase of n2. This is because the increase of the roll speed will lead to an increase of the fluidity of the rolled metal, which will increase the additional deformation of the metal, resulting in the increase of the outer diameter error of the rolled piece. Therefore, under the premise of meeting the rolling bite conditions, selecting a smaller second pass speed is conducive to improving the outer diameter accuracy of the rolled piece.

The roundness error of rolled piece increases with the increase of n2. The roundness errors both are 0.123 mm at 40 rad/min and 60 rad/min. The standard deviation of the wall thickness of the rolled piece increases with the increase of n2, and the change rule is consistent with the roundness error. The smaller second pass roll rotating speed is beneficial to improve the outer diameter roundness and wall thickness uniformity of the rolled piece.

3.5. Effect of Second Pass Axial Speed on Forming Quality

As shown in Figure **10**, the outer diameter error of rolled piece decreases with the increase of the second pass axial velocity(v2). When v2 increases from 10

mm/s to 20 mm/s, the outer diameter error of the rolled piece decreases rapidly from 0.537 mm to 0.307 mm, with a decrease of 0.230 mm. When v2 increases from 20 mm/s to 30 mm/s, the outer diameter error of the rolled piece increases from 0.307 mm to 0.323 mm, and the increase is significantly smaller than the decrease of the outer diameter error from 10 mm/s to 20 mm/s. That is, the outer diameter error of the rolled piece tends to be stable after the axial speed reaches 20 mm/s.
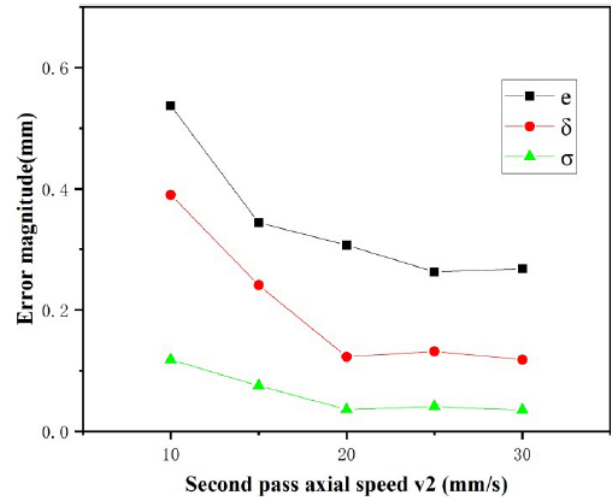

Figure 10: Effects of the second pass axial speed on forming quality.

The roundness error and wall thickness standard deviation of the rolled piece show decreasing trends with the increase of v2, and their minimum values appear at the axial speed of 20 mm/s, which are 0.123mm and 0.036mm, respectively. At this time, the wall thickness of rolled piece is the most uniform. Larger v2 can effectively reduce the roundness error and wall thickness standard deviation of the rolled piece, thereby improving the forming quality of the rolled piece.

3.6. Effects of the Blank Preheating Temperature on Forming Quality

It can be seen from Figure **11** that the outer diameter error of the rolled piece increases with the increase of the preheating temperature of the blank (T). As T increases, the irregular flow of the metal increases, which ultimately affects the outer diameter accuracy of the rolled piece. When T increases from 1000 ºC to 1050 ºC, the outer diameter error increases rapidly, and the increase reaches a maximum of 0.029 mm.

The roundness error of rolled piece decreases first and then increases with the increase of T. When the preheating temperature increases from 950 ºC to 1000 ºC, the roundness error of the rolled piece increases slightly from 0.143 mm to 0.145 mm. When T is 1150 ºC, the roundness error of the rolled piece reaches a maximum of 0.150 mm.

When T increases from 950 ºC to 1000 ºC, the standard deviation of the wall thickness of the rolled piece shows a decreasing trend, but on the whole, it still shows a trend of decreasing first and then increasing with the increase of T, and also reaches the minimum value of 0.036 mm when the preheating temperature is 1000 ºC. According to the analysis, a smaller billet preheating temperature is helpful to improve the stability of metal flow in the rolling process and improve the forming quality.
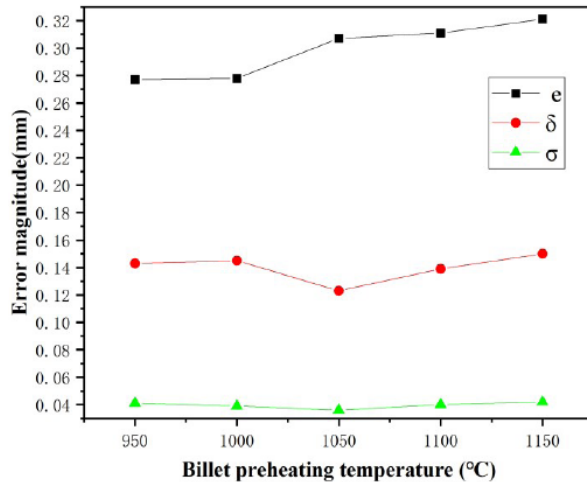

Figure 11: Effects of the blank preheating temperature on forming quality.

Comprehensive comparison of the influence of process parameters in Figures **7~11**, we have obtained the influence law of process parameters on forming quality. It shows that the smaller axial speed and rotational speed should be selected in the first pass of rolling, the larger axial speed and smaller rotational speed should be selected in the second pass of rolling. The parameters of the second pass have more significant influence on the forming quality.

4. PROCESS PARAMETERS OPTIMIZATION

To obtain the best forming quality of the rolled piece, this paper uses the orthogonal test analysis method to optimize the process parameters of the three-roll skew rolling of the turbine shaft, so as to obtain the optimal level combination of the parameters and the order of influence. The numerical simulation is carried out by the optimal parameters to verify the reliability of the orthogonal test.

4.1. Orthogonal Test Program

According to the results of single factor analysis, the orthogonal test scheme of 5 factors and 3 levels was established by selecting the parameters interval with better forming effects. There is a certain interaction between the rotational speed and the axial speed in the rolling process, so the interaction between the two factors is studied as a new factor. The specific factors and level values are shown in Table **5**. The selected five factors are represented by letters A, B, C, D and E respectively.

The author chooses three indexes of outer diameter error, outer roundness error and wall thickness uniformity to measure the forming quality of rolled pieces, and adopts the commonly used ' comprehensive scoring method ' to process the results of multi-index orthogonal test, which is represented by symbol f. Considering that the three indexes selected in this paper have no obvious weight difference, the weight coefficient is set to 1/3. The specific calculation formula is as follows [22]:

$$\Sigma_i = \frac{1}{3}\left(\frac{e_i}{e_{min}} + \frac{\delta_i}{\delta_{min}} + \frac{\sigma_i}{\sigma_{min}}\right) \tag{6}$$

Where Σ_i is the comprehensive score of experiment i; e_i, δ_i, σ_i are the external diameter error, external

Table 5: Test Factor Level Table

Factor \ Levels	n1/rad·min⁻¹ (A)	v1/mm·s⁻¹ (B)	n2/rad·min⁻¹ (C)	v2/mm·s⁻¹ (D)	T/ºC (E)
1	40	15	40	20	1000
2	60	20	50	25	1050
3	80	25	60	30	1100

Table 6:   Orthogonal Test Scheme

No	The Levels of Factor								Error Column				
	A(C×D)	B	A×B		C	D	C×D	E					
1	1	1	1	1	1	1	1	1	1	1	1	1	1
2	1	1	1	1	2	2	2	2	2	2	2	2	2
3	1	1	1	1	3	3	3	3	3	3	3	3	3
4	1	2	2	2	1	1	1	2	2	2	3	3	3
5	1	2	2	2	2	2	2	3	3	3	1	1	1
6	1	2	2	2	3	3	3	1	1	1	2	2	2
7	1	3	3	3	1	1	1	3	3	3	2	2	2
8	1	3	3	3	2	2	2	1	1	1	3	3	3
9	1	3	3	3	3	3	3	2	2	2	1	1	1
10	2	1	2	3	1	2	3	1	2	3	1	2	3
11	2	1	2	3	2	3	1	2	3	1	2	3	1
12	2	1	2	3	3	1	2	3	1	2	3	1	2
13	2	2	3	1	1	2	3	2	3	1	3	1	2
14	2	2	3	1	2	3	1	3	1	2	1	2	3
15	2	2	3	1	3	1	2	1	2	3	2	3	1
16	2	3	1	2	1	2	3	3	1	2	2	3	1
17	2	3	1	2	2	3	1	1	2	3	3	1	2
18	2	3	1	2	3	1	2	2	3	1	1	2	3
19	3	1	3	2	1	3	2	1	3	2	1	3	2
20	3	1	3	2	2	1	3	2	1	3	2	1	3
21	3	1	3	2	3	2	1	3	2	1	3	2	1
22	3	2	1	3	1	3	2	2	1	3	3	2	1
23	3	2	1	3	2	1	3	3	2	1	1	3	2
24	3	2	1	3	3	2	1	1	3	2	2	1	3
25	3	3	2	1	1	3	2	3	2	1	2	1	3
26	3	3	2	1	2	1	3	1	3	2	3	2	1
27	3	3	2	1	3	2	1	2	1	3	1	3	2

roundness error and wall thickness standard deviation of group i experiment respectively.

Due to the interaction between factors, this paper selects $L_{27}(3^{13})$ orthogonal table with interaction, and in strict accordance with the orthogonal table for each analysis factor arrangement [23], as shown in Table **6**.

The comprehensive scores of 27 groups of test results shown in Table **7** were calculated by using the above scoring formula.

Table 7:   Orthogonal Test Results

No	e(mm)	δ(mm)	σ((mm)	Fraction ∑
1	0.187	0.124	0.040	1.124
2	0.215	0.132	0.035	1.160
3	0.267	0.196	0.058	1.665
4	0.164	0.134	0.042	1.120
5	0.242	0.158	0.050	1.432

6	0.243	0.133	0.040	1.271
7	0.228	0.150	0.046	1.341
8	0.254	0.132	0.039	1.283
9	0.325	0.146	0.044	1.524
10	0.152	0.131	0.040	1.066
11	0.231	0.164	0.052	1.443
12	0.293	0.133	0.040	1.381
13	0.197	0.173	0.051	1.383
14	0.239	0.156	0.045	1.372
15	0.278	0.145	0.041	1.390
16	0.278	0.166	0.049	1.523
17	0.222	0.151	0.047	1.340
18	0.34	0.148	0.047	1.598
19	0.269	0.178	0.053	1.573
20	0.184	0.164	0.046	1.282
21	0.242	0.125	0.036	1.210
22	0.263	0.154	0.047	1.438
23	0.246	0.147	0.044	1.354
24	0.264	0.152	0.045	1.416
25	0.552	0.228	0.163	3.376
26	0.222	0.147	0.040	1.263
27	0.267	0.144	0.042	1.373
Average	0.254	0.152	0.049	--

4.2. Discuss

The comprehensive scores in Table **7** are imported into Matlab software for range analysis to obtain the analysis results shown in Table **8**, where T1, T2 and T3 are expressed as the sum of all corresponding test indexes when taking 1,2 and 3 levels in a column, and t1, t2 and t3 are the average values of the corresponding test indexes. The calculation formula is as follows：

$$t_i = \frac{T_i}{r} \tag{7}$$

Where r is the number of occurrences of each level in a column, and the value is 9.

The smaller the comprehensive score, the better the forming quality of the rolled piece, so the level corresponding to the minimum T or t value is the optimal level. According to the data in Table **8**, the optimal level combination of each factor is determined to be A1B1C2D2E1, that is, the first pass roll rotating speed is 40 rad/min, the first pass axial speed is 15 mm/s, the second pass roll rotating speed is 50 rad/min, the second pass axial speed is 25 mm/s, and the billet preheating temperature is 1000 ºC.

The range R is the difference between the maximum and minimum values of the test indexes at each level of the factor, which is used to reflect the change range of the test indexes with the level of the factor. Therefore, the primary and secondary order of the influence of each process parameter on the forming quality of the rolled piece can be obtained according to the size of its value, that is, D>E>B>C×D>A>C>A×B, as shown in Table **8**. Among them, the axial speed of the second pass has the greatest influence on the test results, while the rotational speed of the second pass has the least influence. When considering the interaction, the influence of the matching of the second roll rotating pass speed and the axial speed on the forming quality of the rolled piece is greater than that of the first pass, indicating that the selection of process parameters in the second pass rolling is more

Table 8: Range Analysis Table

Factors	A(C×D)	B	A×B		C	D	C×D	E	Vacant Column
T1	11.920	11.904	12.618	14.106	13.944	11.853	11.739	11.726	—
T2	12.496	12.176	13.725	12.349	11.929	11.846	14.631	12.321	—
T3	14.285	14.621	12.358	12.246	12.828	15.002	12.331	14.654	—
t1	1.324	1.323	1.402	1.567	1.549	1.317	1.304	1.303	—
t2	1.388	1.353	1.525	1.372	1.325	1.316	1.626	1.369	—
t3	1.587	1.625	1.373	1.361	1.425	1.667	1.370	1.628	—
Range （R）	2.365	2.717	1.6135		2.015	3.156	2.6285	2.928	—
Optimum levels	1(1)	1	3	3	2	2	1	1	—
Significance of factor	D>E>B>C×D>A>C>A×B								

important and needs to be given priority in the actual production proces.

4.3. Simulation Verification and Analysis of Optimal Parameters

Through orthogonal test analysis, the optimum process parameters of three-roll skew rolling forming turbine shaft are obtained as follows: the first pass roll rotating speed is 40 rad/min, the first pass axial speed is 15 mm/s, the second pass roll rotating speed is 50 rad/min, the second pass axial speed is 25 mm/s, and the billet preheating temperature is 1000ºC. The optimum temperature for forming Gh4169 shaft parts by cross wedge rolling process is 950 °C, and the grain size is higher at 1000 °C, which has a deviation of 50 °C from the results of this paper [24].

Table 9： **Simulation Results of Optimal Parameter Combination**

Forming Quality Index	Value
e/mm	0.151
δ/mm	0.121
σ/mm	0.034

As shown in Table **9**, the results of the three indexes under the optimal parameter combination are less than all the corresponding indexes in Table **7**, indicating that the outer diameter size, outer surface roundness and wall thickness uniformity of the rolled piece are optimized under this parameter condition, thus verifying the reliability of the orthogonal test design and analysis. According to the comparison of the average values of 27 groups of experimental data, under the optimal process parameters, the outer diameter error of the formed part is reduced by 40.5%, the outer roundness error is reduced by 20.39%, and the wall thickness uniformity is increased by 30.6%.

Based on the numerical simulation results under the optimal parameter combination, the forming quality of the rolling step is explored in detail according to the point selection method in Figure **6**. Figure **12** shows the cross-section forming quality change curves, and the abscissa cross-section serial number is the cross-section order of the rolled piece from left to right in Figure **6**(**a**). It can be seen from Figure **12**(**a**) that there is no obvious fluctuation in the outer diameter error of the first six sections of the Φ42 and Φ35 steps of the rolled piece, but the outer diameter error of the end sections (section 7 and section 14) of the two steps increases significantly. These two sections are close to

the area of the rolled piece under the pressure of the roll, so more reflow metal will be generated during the rolling process, resulting in an increase in the outer diameter of the section. The 16th and 17th sections are located in the middle of the Φ30 step, and the errors are -0.213 mm and -0.235 mm, respectively, that is, the necking phenomenon occurs.
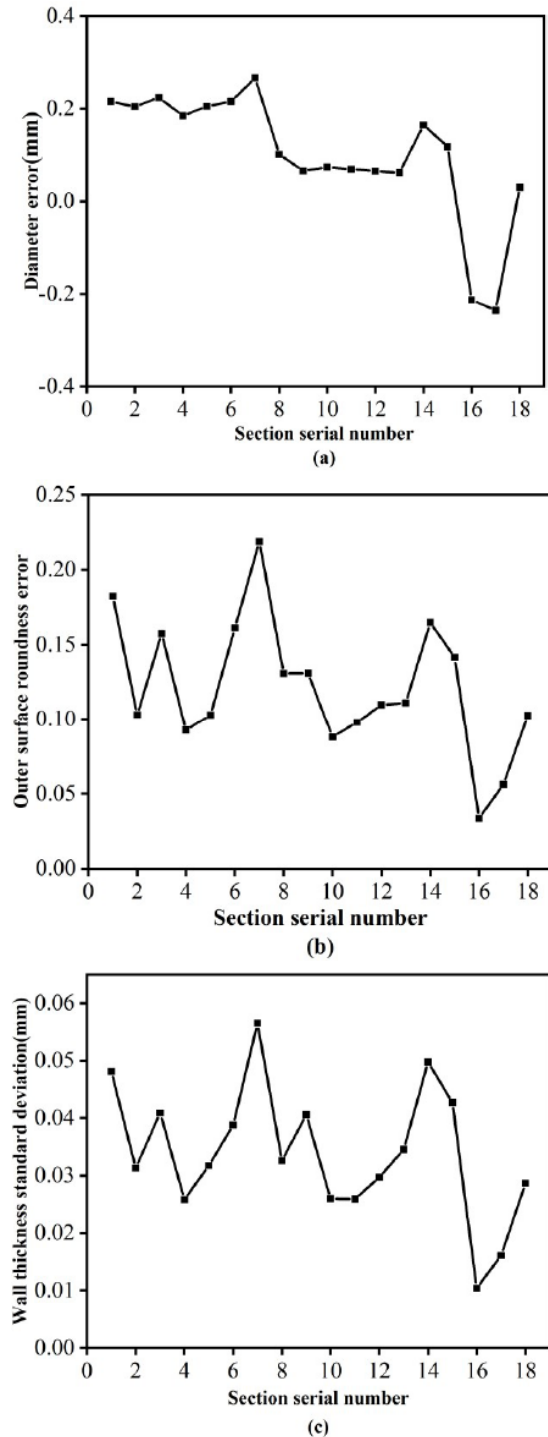

Figure 12: Changes of section forming quality (**a**) Diameter error, (**b**) Outer surface roundness error and (**c**) Wall thickness uniformity.

It can be seen from Figure **12** (**b**) and (**c**) that the variation trend of the external roundness error and the wall thickness standard deviation of the rolled piece section is basically consistent. The maximum values of the Φ42 and Φ35 steps are located at the last section of the two steps. The maximum values of the roundness error and the wall thickness standard deviation of the Φ42 step are 0.219 mm and 0.057 mm respectively, and the maximum values of the Φ35 step are 0.165 mm and 0.050 mm respectively.

Different from the outer diameter error, the roundness error and wall thickness standard deviation of the 16th and 17th cross-sections on the rolled piece are smaller than those of the remaining cross-sections. Because the metal in this area is subjected to axial tensile stress and flows along the axial direction, the additional deformation of the metal is reduced, so the two sections at the necking position have better roundness and wall thickness uniformity.

The average values of the roundness error and wall thickness standard deviation of the three steps of Φ42 mm, Φ35 mm and Φ30 mm are taken respectively. The average values of the roundness error and wall thickness standard deviation of the Φ42 mm step are 0.145 mm and 0.039 mm, the average values of the Φ35mm step are 0.119 mm and 0.034 mm, and the average values of the Φ30mm step are 0.083mm and 0.024 mm. The results are in line with the law that the smaller the forming diameter, the better the forming quality of the rolled piece.

4. CONCLUSION

In this paper, the finite element model of GH4169 superalloy multi-step hollow turbine shaft three-roll skew rolling was established by SF software. The effects of process parameters on the forming quality of rolled parts are explored, and the process parameters are optimized. The main conclusions are as follows:

The influence of process parameters on the forming quality (outer diameter error, outer roundness error and wall thickness uniformity) of the rolled piece is as follows: appropriately increasing the first pass roll rotating speed and the second pass axial speed, reducing the first pass axial speed, the second pass roll rotating speed and the billet preheating temperature can effectively reduce the outer diameter error; Properly increasing the axial speed of the first pass, the axial speed of the second pass and the billet preheating temperature, and reducing the roll rotating

speed of the first pass and the second pass can effectively reduce the roundness error and improve the uniformity of wall thickness.

Based on the orthogonal test method, the process parameters of the three-roll skew rolling of the turbine shaft were optimized, and the optimal process parameter combination was obtained as follows: the first pass roll rotating speed was 40 rad/min, the first pass axial speed was 15 mm/s, the second pass speed was 50 rad/min, the second pass axial speed was 25 mm/s, and the billet preheating temperature was 1000 ºC. Forming by the above parameters, the outer diameter error of the formed part is reduced by 40.5%, the outer roundness error is reduced by 20.39%, and the wall thickness uniformity is increased by 30.6%.

The axial speed of the second pass has the greatest influence on the test results, while the rotational speed of the second pass has the least influence. When considering the interaction, the effect of the combination of the second pass rotational speed and the axial speed on the forming quality is greater than that of the first pass.

The research results in this paper provide a theoretical basis for improving the quality of multi-step hollow turbine shafts of superalloy formed by three-roll skew rolling and realizing flexible and economical high-quality forming of hollow turbine shaft by three-roll skew rolling.

ACKNOWLEDGMENTS

REFERENCES

[1]   Pater Z, Wójcik Ł, Walczuk P. Comparative Analysis of Tube Piercing Processes in the Two-Roll and Three-Roll Mills. Advances in Science and Technology Research Journal 2019; 13(1): 37-45.
https://doi.org/10.12913/22998624/102766

[2]   Nakasuji K, Kuroda K, Hayashi C. Reduce Rolling Characteristics of Hollow Piece by Rotary Rolling Mill. Isij International 1996; 36(5): 572-578.
https://doi.org/10.2355/isijinternational.36.572

[3]   Pater Z, Bulzak T, Tomczak J. Numerical Analysis of a Skew Rolling Process for Producing a Stepped Hollow Shaft Made

of Titanium Alloy Ti6Al4V. Archives of Metallurgy & Materials 2016; 61(2): 677-682.
https://doi.org/10.1515/amm-2016-0115

[4]   Pater Z. FEM Analysis of Loads and Torque in a Skew Rolling Process for Producing Axisymmetric Parts. Archives of Metallurgy and Materials 2017; 62(1): 85-90.
https://doi.org/10.1515/amm-2017-0011

[5]   Stefanik A, Szota P, Mróz S, *et al*. Analysis of the Aluminum Bars in Three-High Skew Rolling Mill Rolling Process. Solid State Phenomena 2015; 220-221: 892-897.
https://doi.org/0.4028/www.scientific.net/SSP.220-221.892

[6]   Stefanik A, Morel A, Mróz S, *et al*. Theoretical And Experimental Analysis Of Aluminium Bars Rolling Process In Three-High Skew Rolling Mill. Archives of Metallurgy & Materials 2015; 60(2): 809-813.
https://doi.org/10.1515/amm-2015-0211

[7]   Min J H, Kwon H C, Lee Y, *et al*. Analytical model for prediction of deformed shape in three-roll rolling process. Journal of Materials Processing Technology 2003, 140(1-3): 471-477.
https://doi.org/10.1016/S0924-0136(03)00717-9

[8]   Lu Q G, Xu W J, Qin Zi. Analysis on wall thickness eccentricity of three-roll rolled hollows of seamless steel tube. Iron & Steel 2020; 55(10): 50-55.
https://doi.org/10.13228/j.boyuan.issn0449-749x.20200042

[9]   Gryc A, Bajor T, Dyja H. The analysis of influence the parameters of rolling process in three high skew rolling mill of AZ31 magnesium alloy bars on temperature distribution. Metalurgija 2016; 55(4): 772-774.

[10] Li S Z, Wang S H, Yin Y D. Influence of Feed Angle on Sizing Reduction During Three-roll Cross Rolling Sizing. Hot Working Technology 2016; 45(1): 155-158.
https://doi.org/10.14158/j.cnki.1001-3814.2016.01.043

[11] Ding X F, Shuang Y H, Shi Y P. Study on Process Parameters of Skew Rolling Piercing of Magnesium Alloy. Hot Working Technology 2017; 46(19): 146-149.
https://doi.org/10.14158/j.cnki.1001-3814.2017.19.039

[12] Wang Y L, Hu Z Q, Wang K K. Numerical simulation and processing parameter optimization of the double-layer stainless steel tube by three-roll cross rolling. Steel Rolling 2018; 35(06): 39-44.
https://doi.org/10.13228/j.boyuan.issn1003-9996.20170164

[13] Shu X D, Zhang S, Shu C, *et al*. Research and prospect of flexible forming theory and technology of hollow shaft by three-roll skew rolling. The International Journal of Advanced Manufacturing Technology (2022).
https://doi.org/10.1007/s00170-022-10242-y

[14] Li G Y. Research on thinning forming process of superalloy GH4169 welded pipe[D]. Shenyang University of Technology; 2016.

[15] Wu H, Kong X W. Luo P. Constitutive Equation for High-Temperature Deformation of GH4169 Alloy. Machinery Design & Manufacture 2020; (08): 163-167.
https://doi.org/10.19356/j.cnki.1001-3997.2020.08.038

[16] Li S Z, Duan X G, Yin Y D, *et al*. Influence of Variable Guide Disc-fore on Force Parameters and Expanding Diameter in Rotary Piercing Process. Journal of Anhui University of Technology (Natural Science) 2009; 26(01): 27-31.

[17] Hu Z. Recent progress on the finite element simulation techniques of metal forming processes. Journal of plasticity engineering 1994; 1(03): 3-13.

[18] Xu Y M, Sun B S, Shu X D, *et al*. Numerical simulation of multi-step turbine shaft in three-roll screw rolling on its influence by diameter reduction. Journal of Ningbo University (Natural Science & Engineering Edition) 2021; 34(04): 55-60.

[19] Sukhorukov R Y, Sidorov A A, Alimov A I, *et al*. Physical and numerical modeling of the process of rolling off of a tapered shaft of aviation purpose. Journal of Machinery Manufacture and Reliability 2016; 45(6): 538-545.
https://doi.org/10.3103/S1052618816060121

[20] Chen Y, Xia Y, Bian Y, *et al*. Image measurement of precision aluminum alloy forgings. Journal of Plasticity Engineering 2010; 17(6): 77-81.

[21] Zhou J. Finite element simulation of multi-pass reversible hot rolling of high temperature alloy steel plate[D]. Shanghai Jiao Tong University 2009.

[22] Wang C W. Research on Cold Rolling Forming Technology of Bimetallic Composite Bearing Ring[D]. Ningbo University, 2018.

[23] Zhao Z Q. Research on Asymmetric Cold Rolling Forming Technology of Inner Ring of High Speed Railway Bearing[D]. Ningbo University 2017.

[24] Zhu D B. Research on Macroscopic and Microscopic Law of GH4169 Superalloy Shaft Parts by Cross Wedge Rolling Ningbo University 2019.
https://doi.org/10.27256/d.cnki.gnbou.2019.000930.